U.S. Army Medical Research
Institute of Chemical Defense

USAMRICD-TR-08-03

Electrophysiological and Ultrastructural Characterization of Neuromuscular Junctions in Diaphragm Muscle of Acetylcholinesterase Knockout Mice

Michael Adler
Tracey A. Hamilton
Oksana Lockridge
Ellen Duysen
Sharad S. Deshpande[a]

April 2008

U.S. Army Medical Research
Institute of Chemical Defense
Aberdeen Proving Ground, MD 21010-5400

DISPOSITION INSTRUCTIONS:

Destroy this report when no longer needed. Do not return to the originator.

DISCLAIMERS:

The opinions, interpretations, conclusions, and recommendations are those of the author and are not necessarily endorsed by the U.S. Army or the Department of Defense.

The experimental protocol was approved by the Animal Care and Use Committee at the United States Army Medical Research Institute of Chemical Defense and all procedures were conducted in accordance with the principles stated in the Guide for the Care and Use of Laboratory Animals (National Research Council, Publication No. 85-23, 1996), and the Animal Welfare Act of 1966 (P.L. 89-544), as amended.

The use of trade names does not constitute an official endorsement or approval of the use of such commercial hardware or software. This document may not be cited for purposes of advertisement.

REPORT DOCUMENTATION PAGE

Form Approved
OMB No. 0704-0188

1. REPORT DATE *(DD-MM-YYYY)*	**2. REPORT TYPE**	**3. DATES COVERED** *(From - To)*
April 2008	Technical Report	January 2005 – December 2007

Electrophysiological and Ultrastructural Characterization of Neuromuscular Junctions in Diaphragm Muscle of Acetylcholinesterase Knockout Mice

5a. CONTRACT NUMBER

5b. GRANT NUMBER

5c. PROGRAM ELEMENT NUMBER

6. AUTHOR(S)
Adler, M, Hamilton, TA, Lockridge, O*, Duysen, E* and Deshpande, SS

5d. PROJECT NUMBER

5e. TASK NUMBER
6.1

5f. WORK UNIT NUMBER

7. PERFORMING ORGANIZATION NAME(S) AND ADDRESS(ES)

US Army Medical Research Institute of Chemical Defense
ATTN: MCMR-CDT-N
3100 Ricketts Point Road
Aberdeen Proving Ground, MD 21010-5400

8. PERFORMING ORGANIZATION REPORT NUMBER

USAMRICD-TR-08-03

9. SPONSORING / MONITORING AGENCY NAME(S) AND ADDRESS(ES)

US Army Medical Research Institute of Chemical Defense
ATTN: MCMR-CDZ-P
3100 Ricketts Point Road
Aberdeen Proving Ground, MD 21010-5400

10. SPONSOR/MONITOR'S ACRONYM(S)

11. SPONSOR/MONITOR'S REPORT NUMBER(S)

12. DISTRIBUTION / AVAILABILITY STATEMENT

Approved for public release; distribution unlimited

13. SUPPLEMENTARY NOTES

* Eppley Institute, University of Nebraska Medical Center, Omaha, NE 68198 USA

14. ABSTRACT

Electrophysiological and ultrastructural studies were performed on phrenic nerve-hemidiaphragm preparations isolated from wild-type (AChE +/+) and acetylcholinesterase knockout (AChE -/-) mice to determine the compensatory mechanism manifested by the neuromuscular junction to excess acetylcholine (ACh). Nerve-elicited muscle contractions, miniature endplate potentials (MEPPs) and evoked endplate potentials (EPPs) were recorded by conventional electrophysiological techniques from phrenic nerve-hemidiaphragm preparations isolated from 1.5- to 2-month-old mice. Tension measurements from AChE -/- mice revealed that the amplitude of twitch tensions was potentiated, but tetanic tensions underwent a use-dependent decline at frequencies below 70 Hz and above 100 Hz. MEPPs in AChE -/- diaphragms showed a slight reduction in amplitude (20%) and a small prolongation in decay (26%) relative to values observed in wild-type mice. In contrast, MEPPs recorded from AChE +/+ diaphragms exposed for 30 min to the selective AChE inhibitor 5-bis(4-allyldimethyl-ammoniumphenyl)pentane-3-one (BW284C51) exhibited a pronounced increase in amplitude (63%) and a marked prolongation in decay (115%). The difference between MEPP amplitudes and decays in AChE -/- diaphragms and in AChE +/+ diaphragms treated with BW284C51 represents effective adaptation by the former to a high ACh environment. Electron microscopic examination revealed that diaphragm muscles of AChE -/- mice had smaller nerve terminals and diminished pre- and postsynaptic surface contacts relative to neuromuscular junctions of AChE +/+ mice. The morphological changes are suggested to account, in part, for the ability of muscle from AChE -/- mice to function in the complete absence of AChE.

15. SUBJECT TERMS

Neuromuscular junction; Acetylcholinesterase; Butyrylcholinesterase; Knockout; Mouse diaphragm; Electron microscopy; Electrophysiology

16. SECURITY CLASSIFICATION OF:			**17. LIMITATION OF ABSTRACT**	**18. NUMBER OF PAGES**	**19a. NAME OF RESPONSIBLE PERSON**
a. REPORT	**b. ABSTRACT**	**c. THIS PAGE**			Michael Adler
UNCLASSIFIED	UNCLASSIFIED	UNCLASSIFIED	UNLIMITED	20	**19b. TELEPHONE NUMBER** *(include area code)* 410-436-1913

Abstract

Electrophysiological and ultrastructural studies were performed on phrenic nerve-hemidiaphragm preparations isolated from wild-type (AChE +/+) and acetylcholinesterase knockout (AChE -/-) mice to determine the compensatory mechanism manifested by the neuromuscular junction to excess acetylcholine (ACh). The diaphragm was selected since it is the primary muscle of respiration, and it must adapt to allow for survival of the organism in the absence of AChE. Nerve-elicited muscle contractions, miniature endplate potentials (MEPPs) and evoked endplate potentials (EPPs) were recorded by conventional electrophysiological techniques from phrenic nerve-hemidiaphragm preparations isolated from 1.5- to 2-month-old mice. These recordings were chosen to provide a comprehensive assessment of functional alterations of the diaphragm muscle resulting from the loss of AChE. Tension measurements from AChE -/- mice revealed that the amplitude of twitch tensions was potentiated, but tetanic tensions underwent a use-dependent decline at frequencies below 70 Hz and above 100 Hz. MEPPs in AChE -/- diaphragms showed a slight reduction in amplitude (20%) and a small prolongation in decay (26%) relative to values observed in wild-type mice. In contrast, MEPPs recorded from AChE +/+ diaphragms that were exposed for 30 min to the selective AChE inhibitor 5-bis(4-allyldimethyl-ammoniumphenyl)pentane-3-one (BW284C51) exhibited a pronounced increase in amplitude (63%) and a marked prolongation in decay (115%). The difference between MEPP amplitudes and decays in AChE -/- diaphragms and in AChE +/+ diaphragms treated with BW284C51 represents effective adaptation by the former to a high ACh environment. Electron microscopic examination revealed that diaphragm muscles of AChE -/- mice had smaller nerve terminals and diminished pre- and postsynaptic surface contacts relative to neuromuscular junctions of AChE +/+ mice. The morphological changes are suggested to account, in part, for the ability of muscle from AChE -/- mice to function in the complete absence of AChE.

1. Introduction

Neuromuscular transmission is initiated by depolarization of the presynaptic membrane and culminates in the synchronous release of acetylcholine (ACh) from small synaptic vesicles (SSVs) docked at active zones (Heuser et al., 1979). ACh then diffuses across the synaptic cleft and combines with binding sites on two α subunits of the pentameric nicotinic ACh receptor (AChR), leading to the opening of the associated ligand-gated ion channel (Karlin, 2002). Channel opening triggers, in turn, the endplate current (EPC), endplate potential (EPP), muscle action potential and muscle contraction (Miyazawa et al., 2003). Normal operation of the neuromuscular junction requires removal of ACh within several msec of receptor activation to allow for sustained high frequency firing: otherwise persistence of ACh would lead to membrane depolarization, retrograde firing, receptor desensitization, muscle fasciculation and muscle weakness (Katz and Miledi, 1973; Heffron and Hobbiger, 1979; Magleby and Pallotta, 1981). Removal of ACh is accomplished by hydrolysis to choline and acetate, neither of which has appreciable agonist action at the neuromuscular junction (Akk et al., 2005).

There are two enzymes capable of hydrolyzing ACh: acetylcholinesterase (AChE) and butyrylcholinesterase (BChE). AChE is the primary hydrolytic enzyme and produces rapid cleavage of ACh (Zimmerman and Soreq, 2006; Colletier et al., 2006). At the neuromuscular junction, under normal conditions, BChE has an insignificant role in hydrolysis of ACh due its lower cleavage rate (Chatonnet and Lockridge, 1989; Brimijoin and Koenigsberger, 1999). However, BChE has been suggested to participate in the hydrolysis of ACh in other systems, such as airway smooth muscle, that function on a slower time scale (Adler et al., 1991). Much of our information on the role of AChE in synaptic transmission has come from use of selective AChE inhibitors such as 1,5-bis(4-allyldimethyl-ammoniumphenyl)pentane-3-one (BW284C51), huperzine, galantamine, rivastigmine, and fasciculin (Bois et al., 1980; Rosenberry et al., 1999; Albuquerque et al., 2006). While these studies have shed light on the consequences of impaired ACh hydrolysis, interpretation of data is often complicated by incomplete inhibition, imperfect selectivity and unrelated "direct" actions of the agents (Bois et al., 1980; Fiekers, 1985; Adler et al., 1991).

An alternative approach is to study neuromuscular transmission in a line of AChE knockout mice (AChE -/-) developed in the laboratory of Dr. Lockridge (Xie et al., 2000; Li et al., 2000). These mice fail to express AChE, but produce normal levels of both soluble and asymmetric forms of BChE. AChE -/- mice have been found to exhibit low body weight and an exaggerated startle response. In addition they manifest fine motor tremors, pinpoint pupils, circling gait and generalized muscle weakness (Duysen et al., 2001). In spite of these abnormalities, AChE -/- mice have a life expectancy of over 3 months, and some are able to live to adulthood, when maintained on a nutritionally balanced liquid diet (Duysen et al., 2002; Minic et al., 2003). The ability of these mice to survive is remarkable since acute inhibition of AChE leads to death within several min. Inhibition of ACh is, in fact, the primary mechanism of the highly lethal nerve agents (Taylor, 1991).

In a previous study, we found that endplates from AChE -/- mice exhibited a marked reduction of AChRs as revealed by fluorescent α-bungarotoxin binding (Adler et al., 2004). A decrease in AChR density would have the effect of reducing transmitter accumulation by allowing ACh elimination to approach free diffusion limits (Katz and Miledi, 1973; Magleby and Pallotta, 1981; Girard et al., 2007). To shed further light on the alterations in neuromuscular

structure and function, we studied the consequences of loss of AChE on diaphragmatic tensions in response to supramaximal stimulation of the phrenic nerve, on miniature endplate potentials (MEPPs) and EPPs by electrophysiological techniques and on synaptic ultrastructure by transmission electron microscopy (TEM). Repetitive indirect stimulation of diaphragm muscles from AChE -/-mice led to tetanic fade at frequencies ≤ 50 Hz and ≥ 200 Hz but to sustained tension at 70 and 100 Hz. Electrophysiological recordings revealed that the probability of release of ACh (*m*) was close to normal in AChE -/- mice, despite the complete absence of AChE. Moreover, MEPP amplitudes and decays were only slightly altered, and MEPP frequencies were unchanged from those recorded from diaphragm muscles of wild-type mice. TEM studies indicated extensive synaptic remodeling consisting of reductions in nerve terminal size and of postjunctional surface area. These ultrastructural alterations, in conjunction with a reduced receptor density and maintained BChE activity reported earlier (Adler et al., 2004), may be responsible for the near-normal neuromuscular transmission in AChE -/- mice.

2. Materials and Methods

2.1 Animal Preparation

Wild-type 129SVJ mice (AChE +/+) and nullizygous AChE -/- mice of either sex were obtained from the University of Nebraska Medical Center and housed at the USAMRICD under an AAALAC accredited animal care and use program. AChE -/- mice were maintained on Ensure fiber™ in sterile petri dishes (8 ml/mouse per 24-hr period), while AChE +/+ mice were provided with commercial rodent ration. Both AChE +/+ and AChE -/- mice had access to tap water *ad libitum*. Animal holding rooms were maintained at 70 ± 2° F with 50 ± 10% relative humidity using at least 10 complete changes per hour of 100% conditioned fresh air. The mice were on a 12-hr light/dark full-spectrum lighting cycle. AChE +/+ and AChE -/- mice were 58.7 ± 2.9 and 51.6 ± 3.2 days old and weighed 33.9 ± 2.8 g and 19.1 ± 0.81 g, respectively, at the time of sacrifice. Mice were euthanatized by exposure to excess CO_2, and diaphragms were excised and pinned at resting length in Sylgard™ (Dow Chemical Co., Midland, MI) coated dishes containing oxygenated Krebs-Ringer solution of the following composition (mM): NaCl, 145; KCl, 5.4; $CaCl_2$, 1.8; $MgCl_2$, 1.0; $NaHCO_3$, 15; NaH_2PO_4, 1.0; glucose, 11.0. The solution was bubbled with a gas mixture of 95% O_2 and 5% CO_2 and had a pH of 7.3-7.4. Diaphragm muscles were split at the central tendon to provide 2 hemidiaphragms with independent nerve supply, and they were prepared for tension recordings or microelectrode impalements, as appropriate.

2.2 Contractility measurements

Hemidiaphragms with attached phrenic nerves were mounted in tissue baths at 37° C and immersed in an oxygenated Krebs-Ringer solution. To obtain single twitches, the phrenic nerve was stimulated supramaximally (5-7 V) with 0.2-msec pulses at 0.03 Hz. The response of muscles to repetitive stimulation was probed by eliciting 500-msec long trains at frequencies of 20, 50, 70, 100, 200 and 400 Hz. To avoid neuromuscular fatigue, trains were elicited at a low duty cycle (2 trains per min). Muscle twitches were measured with an isometric force transducer (FORT 10, WP Instruments, Sarasota, FL) and analyzed off-line with pClamp 8.0 software (Molecular Devices, Boston, MA). Resting tensions were adjusted to 0.5 g to obtain optimal twitch tensions. The parameters measured were peak tension (g), 10-90% rise time (msec) and 90-10% relaxation time (msec).

2.3 Intracellular Microelectrode Techniques

MEPPs and EPPs were recorded at 35 - 37° C from surface fibers of AChE +/+ and AChE -/- hemidiaphragms using standard electrophysiological techniques. Muscle fibers were impaled near endplate regions with borosilicate glass microelectrodes filled with 3 M KCl (15-20 MΩ). Criteria for successful impalement consisted of MEPPs with rise times ≤ 1 msec and stable resting potentials of ≥ -65 mV. At least 100 MEPPs were recorded from each muscle fiber. Quantal content of the EPP (*m*) was determined by method of failures (Del Castillo and Katz, 1954). EPPs were elicited by supramaximal stimulation at a frequency of 0.03 Hz applied to the phrenic nerve via suction electrodes. Tissues were superfused with a modified Krebs-Ringer solution in which Mg^{2+} was increased to 8 mM and Ca^{2+} was reduced to 1 mM. This solution suppressed muscle action potentials and twitches and allowed the quantal nature of the EPP to be studied. The first 50 responses were used to calculate *m* according to the expression $m = \ln (N/N_f)$, where N is the total number of stimuli and N_f is the number of stimuli that fail to elicit EPPs.

Microelectrode signals were recorded on an Axoclamp-2B amplifier (Molecular Devices, Union City, CA) and analyzed off-line with pClamp 8.0 software (Molecular Devices). The parameters measured were peak amplitude, frequency, 10-90% rise time and 90-10% decay time. A threshold detector was positioned at 50% above baseline to allow for capture of the smallest MEPPs while avoiding noise spikes. Data were obtained from 18-26 muscle fibers in 4-6 AChE +/+ and 4-5 AChE -/- mice, and are expressed as mean ± SEM.

2.4 Data Analysis

Statistical analysis was performed by the two-tailed, unpaired Students t-test using InStat (Graphpad, San Diego, CA). A P value ≤ 0.05 was considered to be statistically significant.

2.5 TEM Procedures

Diaphragm muscles were fixed by immersion in buffered 1.6% formaldehyde/2.5% glutaraldehyde at 4° C. After incubation for 24 hr, muscles were washed 3 times for 15 min each in 0.1 M Na cacodylate buffer (pH 7.4, 194 mOsm/Kg) and post-fixed for 30 min in buffered 1% osmium tetroxide. Tissues were dehydrated through graded ethanol and bathed in propylene oxide for two 15-min periods. This was followed by addition of Poly/bed 812® resin and propylene oxide at ratios (w/w) of 1:1 and 1:3 for 2 hr each and by incubation in pure Poly/bed resin overnight under vacuum. Tissues were flat embedded and polymerized at 60° C for 24 hr. Semithin sections were used for preliminary morphological assessment and to select areas of interest for TEM. Ultrathin tissue sections for TEM were collected on copper mesh supporting grids and counterstained using uranyl acetate and lead citrate. Observations were performed using a JEOL 1200EX electron microscope.

2.6 Reagents

Poly/Bed 812®, propylene oxide (electron microscopy grade) and sodium cacodylate were from Polyscience, Inc., Warrington, PA. Glutaraldehyde, paraformaldehyde, and osmium tetroxide (all TEM grade) were purchased from Electron Microscopy Sciences, Ft. Washington, PA. BW284C51 and iso-OMPA and all other reagents were from Sigma-Aldrich Corp. (St. Louis, MO).

3. Results

3.1 Contractility Studies

The characteristics of single twitches from isolated diaphragm muscles of AChE +/+ and AChE -/- mice are summarized in Table 1. Diaphragm muscles from AChE -/- mice had twitch tensions with larger amplitudes, and slower rise and decay times than those observed in wild type muscle. The larger amplitudes were unexpected, especially in light of the lower body weight and overall weakness of these animals (Duysen et al., 2002). Spontaneous muscle fasciculations, which were commonly observed in the intact animal, were not detected in the isolated AChE -/- diaphragm muscle, suggesting that these responses originate outside the muscle.

The ability of diaphragm muscles from AChE -/- mice to develop and maintain tetanic tension was probed by recording responses to repetitive stimulation of the phrenic nerve at frequencies ranging from 20-400 Hz. Muscles from wild-type mice maintained tension at these frequencies with little or no decrement (Fig. 1A). Muscles from AChE -/- mice were able to generate sustained tetanic responses at 70 and 100 Hz, but higher or lower stimulation frequencies led to progressive reductions in muscle tension during the 500-msec trains (Fig. 1B). The maintenance of tetanic tensions at 70 and 100 Hz may be a consequence of the relatively slow time course of twitches in AChE -/- mice (Table 1). The latter would allow for more effective summation of tension by enabling tetanic fusion to occur at lower frequencies (50 Hz).

3.2 Synaptic Transmission

Representative MEPPs recorded from AChE +/+ and AChE -/- mice are shown in Fig. 2, and quantal responses averaged from 4-6 muscles are summarized in Table 2. MEPPs represent spontaneous release of ACh from active zones, and their amplitude, frequency and time course reveal important information about alterations of neuromuscular transmission due to loss of AChE. In diaphragm muscle from AChE +/+ mice, MEPPs exhibited a mean amplitude of 1.08 mV, a rise time of 0.83 msec, a decay time of 3.08 msec and a frequency of 1.45 per sec (Table 2). These values are typical for control quantal responses in mammalian skeletal muscle (Del Castillo and Katz, 1954; Yu and Van der Kloot, 1991). MEPPs recorded from diaphragm muscle of AChE -/- mice had similar properties to those observed in wild-type mice (Fig. 2, Table 2). MEPPs from AChE -/- mice had a mean amplitude of 0.86 mV, a rise time of 0.95 msec, a decay time of 4.15 msec and a frequency of 1.51 per sec. Only the amplitude and decay showed significant alterations ($P \leq 0.05$), while rise time and frequency remained within control levels.

To demonstrate the more striking alterations that result from acute inhibition of AChE, we exposed wild-type mice to the selective AChE inhibitor BW284C51. At the concentration used (1 μM), BW284C51 produces a 97.8 ± 0.7 % inhibition of AChE (Adler et al., 2004). Addition of 1 μM BW284C51 to diaphragm muscles from AChE +/+ muscle resulted in a 63% increase in the MEPP amplitude and a 115% increase in its decay time (Fig. 2, Table 2). Addition of

BW284C51 to muscles from AChE -/- mice was without effect, consistent with the absence of AChE in this preparation (Fig. 2, Table 2).

Since AChE -/- mice are able to express BChE (Xie et al., 2000; Li et al., 2000; Minic et al., 2003), hydrolysis of ACh by BChE may contribute to the maintenance of cholinergic function. To examine this possibility, we recorded MEPPs in the presence of the BChE inhibitor iso-OMPA (10 μM). At this concentration, iso-OMPA inhibits 89% of BChE but only 12% of AChE (Adler et al., 2004). If BChE contributes to the hydrolysis of ACh, MEPPs would be expected to show increased amplitudes and prolonged decays in the presence of iso-OMPA similar to those found with BW284C1. The actions of iso-OMPA would be especially prominent in muscles from AChE -/- mice, where BChE is the only enzyme capable of hydrolyzing ACh. As indicated in Fig. 2 and Table 2, however, iso-OMPA failed to alter MEPP amplitudes or decay times in diaphragm muscle from either AChE -/- or wild-type animals. These results make it unlikely that BChE is responsible for the relatively normal amplitude and decay of MEPPs in AChE -/- mice. However, BChE does appear to contribute to the hydrolysis of ACh during repetitive stimulation as evidenced by the finding that iso-OMPA markedly enhanced tetanic fade in diaphragm muscles from these mice during high frequency stimulation ($\geq$ 70 Hz) (Adler et al., 2004).

To determine whether AChE -/- mice exhibit alterations in evoked release, we examined the quantal content of the EPP. Fig. 3 shows superimposed traces of EPPs from diaphragm muscle of AChE +/+ and AChE -/- mice in a high Mg^{2+}/low Ca^{2+} solution. From the ratio of responses/failures, it is possible to determine *m,* the mean number of quanta per stimuli (Del Castillo and Katz, 1954). In AChE +/+ mice, *m* was calculated to be 2.54 ± 0.42 under the present experimental conditions. In muscle from AChE -/- mice, *m* was determined to be 2.26 ± 0.19, a reduction of only 11%, which was not statistically significant. An absence of change in *m* was previously reported by Minic et al. (2003) in AChE -/- mice. Further examination of EPPs between diaphragms of AChE-/- and AChE +/+ mice revealed that there were no differences in latency (time from nerve stimulation to the onset of response) and in rise time, while the decay of the EPP was slightly prolonged (similar to that of the MEPP). These results suggest that evoked synaptic transmission in diaphragm muscle is well-maintained in AChE -/- mice.

3.4 Synaptic ultrastructure

To investigate morphological alterations of endplates from nullizygous diaphragm muscle, we examined neuromuscular junctions in AChE +/+ and AChE -/- mice by TEM. Typical neuromuscular junctions from a control mouse and one from an age-matched AChE -/- mouse are shown in Fig. 4A and 4B, respectively. Neuromuscular junctions from AChE -/- mice exhibited marked abnormalities, including alterations of presynaptic membranes, synaptic clefts and junctional folds (Fig. 4B). Nerve terminals exhibited a smaller surface area and appeared to contain fewer SSVs. Junctional folds were reduced in number and irregular in shape. In addition, Schwann cells, which are normally found on the outer surface of the nerve terminal, were often observed extending into the synaptic cleft. This is clearly illustrated in the inset to Fig. 4B, where a Schwann cell process is positioned between the nerve terminal and the primary synaptic cleft, and in the upper right section of Fig. 4B, where a nerve terminal is completely engulfed by a Schwann cell.

The cumulative effect of these alterations would be to reduce the pre- and postsynaptic contacts and to open additional pathways for diffusion of ACh. These findings are consistent with morphological changes described in patients with a genetic impairment of collagen-tailed AChE (Hutchinson et al., 1993). Significantly, nullizygous endplates did not show swelling of organelles (mitochondria, endoplasmic reticulum) or supercontractions, which are common ultrastructural changes following acute inhibition of AChE (Laskowski et al., 1977; Adler et al., 1992).

TABLE 1

Indirectly elicited single twitches in AChE +/+ and AChE -/- mice[1]

Condition	Amplitude (g)	Rise time (msec)	Relaxation (msec)
AChE +/+	0.9 ± 0.1	7.7 ± 0.5	17.4 ± 0.6
AChE -/-	4.7 ± 0.4[2]	15.9 ± 0.8[2]	24.0 ± 0.9[2]

[1]Data are expressed as mean ± SEM and were obtained from 8-21 AChE +/+ and 9-11 AChE -/- mice. Tensions were elicited by supramaximal stimulation of the phrenic nerve (5-7 V, 0.2 msec)
[2]Differs significantly from control AChE +/+ values, $P \leq 0.05$.

TABLE 2

Characteristics of MEPPs Recorded from Diaphragm Muscles of AChE +/+ and AChE -/- mice[1]

Condition	Amplitude mV	10-90% Rise msec	90-10% Decay msec	Frequency sec^{-1}
AChE +/+	1.08 ± 0.11	0.83 ± 0.05	3.08 ± 0.14	1.45 ± 0.37
BW + AChE +/+	1.76 ± 0.24[2]	0.96 ± 0.17	6.63 ± 0.39[2]	1.79 ± 0.51
IO + AChE +/+	1.03 ± 0.07	0.87 ± 0.21	3.41 ± 0.26	1.28 ± 0.22
AChE -/-	0.86 ± 0.06[2]	0.95 ± 0.11	4.15 ± 0.33[2]	1.51 ± 0.30
BW + AChE -/-	0.82 ± 0.07	0.91 ± 0.09	4.26 ± 0.19	1.22 ± 0.31
IO + AChE -/-	0.79 ± 0.05	0.85 ± 0.14	4.03 ± 0.26	1.31 ± 0.24

[1]Values represent the mean ± S.E. of 18-26 fibers from 4-6 AChE +/+ and 4-5 AChE -/- diaphragm muscles. Muscles were incubated with the selective AChE inhibitor BW248C51 (BW; 1 μM) or iso-OMPA (IO; 10 μM) for 30 min prior to recording. [2]Differs significantly from control AChE +/+ values, $P \leq 0.05$.

Figure 1. Muscle tensions in response to repetitive stimulation of the phrenic nerve in AChE +/+ (A) and AChE -/- (B) diaphragms. Tensions were generated using 500-msec long stimuli to the phrenic nerve at 20, 50, 70, 100, 200 and 400 Hz. The muscle was allowed to rest for 30 sec between trains. Profiles illustrated are typical of diaphragmatic tensions recorded in muscles isolated from 8-21 AChE +/+ and 9-11 AChE -/- mice.

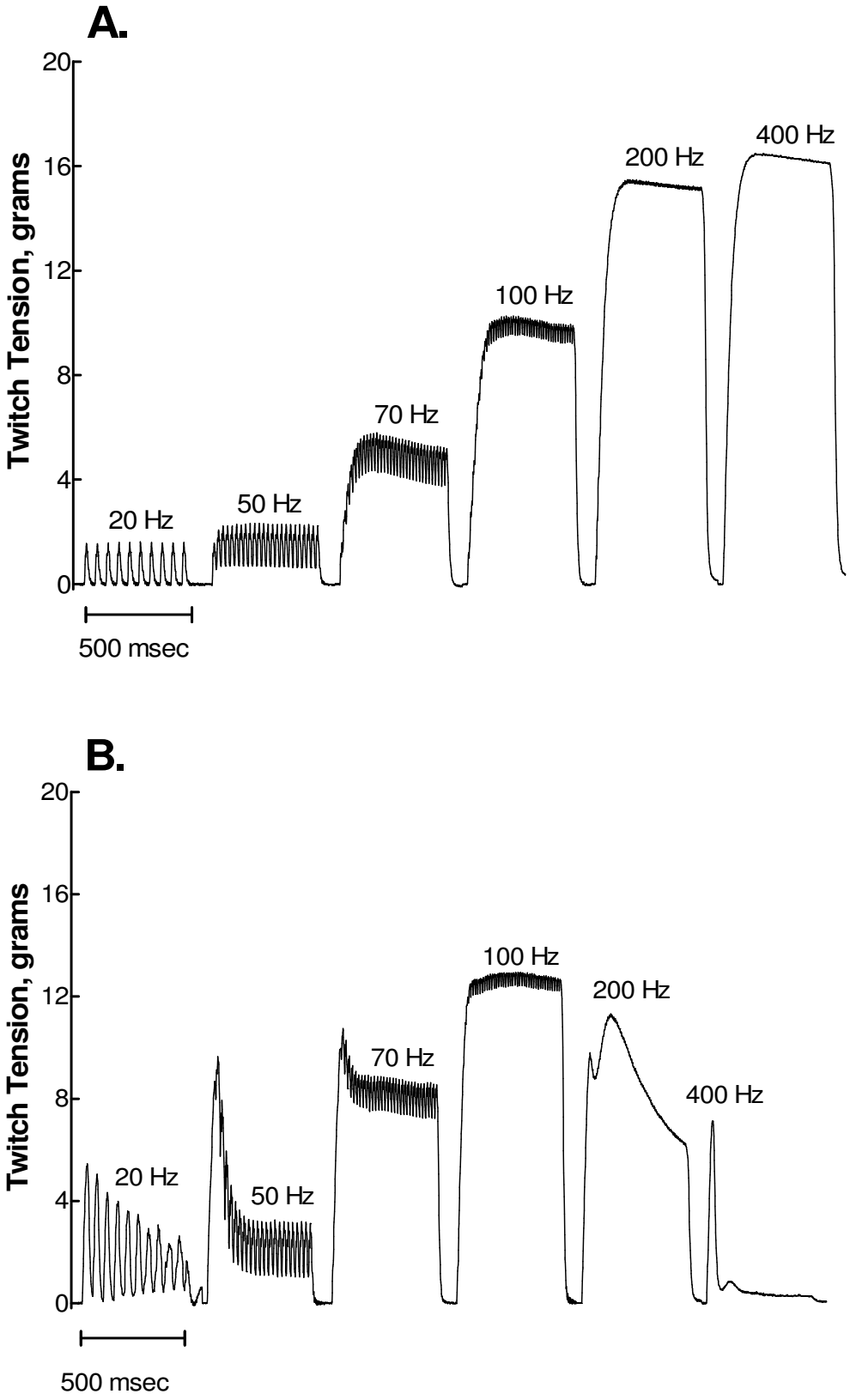
A.
Twitch Tension, grams
20
16
12
8
4
0
20 Hz
50 Hz
70 Hz
100 Hz
200 Hz
400 Hz
500 msec
B.
Twitch Tension, grams
20
16
12
8
4
0
20 Hz
50 Hz
70 Hz
100 Hz
200 Hz
400 Hz
500 msec

Figure 1

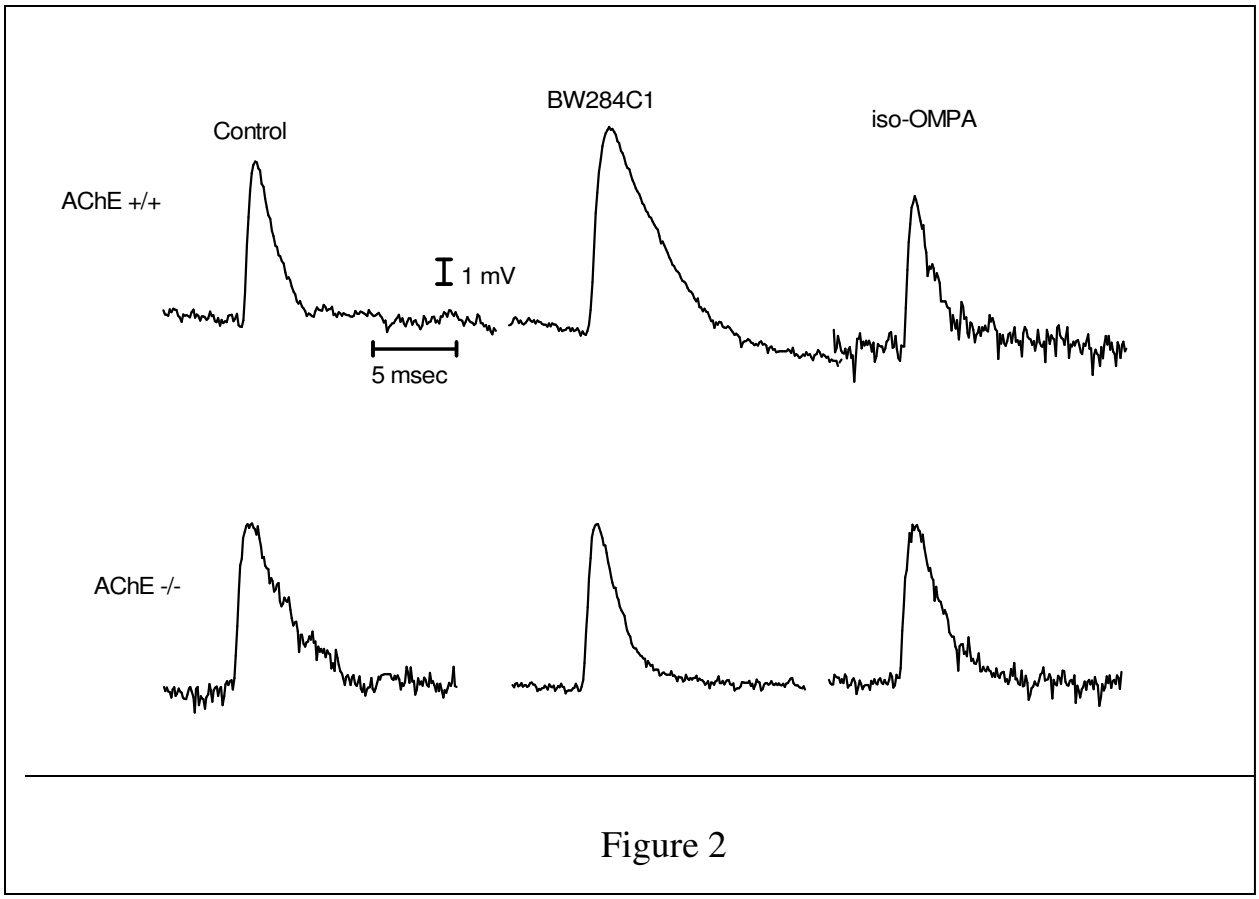

Figure 2

Figure 2. Traces showing MEPPs recorded from surface fibers of diaphragm muscles under control conditions and 30 min after exposure to the selective AChE inhibitor BW 284C51 (1 μM), or the selective BChE inhibitor iso-OMPA (10 μM) in AChE +/+ and AChE -/- mice. Note that BW284C1 increases the amplitude and decay of MEPPs in AChE +/+ but not in AChE -/- diaphragms, and that iso-OMPA has no effect on either muscle. Calibration bars apply to all traces.

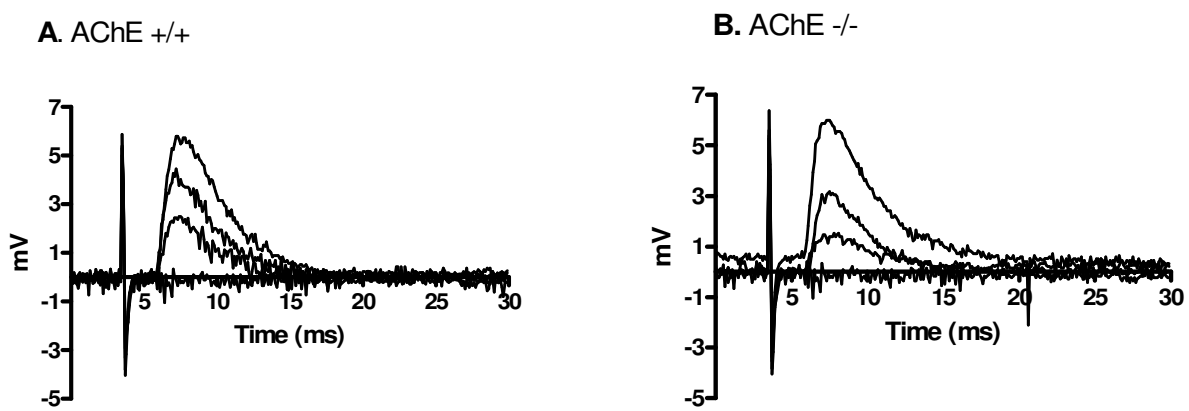

Figure 3

Figure 3. Superimposed traces showing evoked EPPs recorded from the endplate region of diaphragm muscles isolated from (**A**) AChE +/+ and (**B**) AChE-/- mice. EPPs were elicited by supramaximal nerve stimulation in a Krebs-Ringer solution containing 8 mM Mg^{2+} and 1 mM Ca^{2+} to suppress muscle action potentials and twitches. Failure of EPP generation is reflected by the horizontal traces lacking responses. Four superimposed traces are shown for each condition.

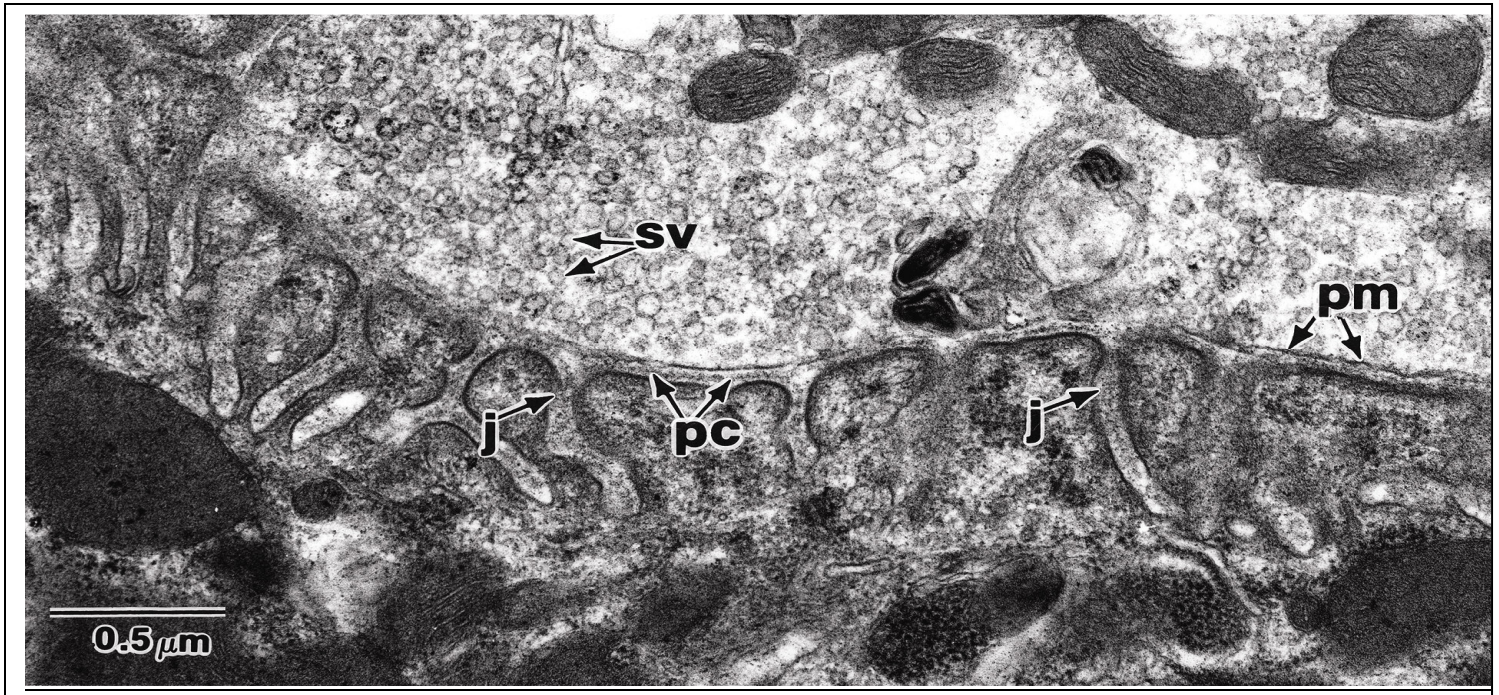

Figure 4a

Figure 4. (**A**) Motor endplate from a diaphragm muscle of an AChE +/+ mouse. Structures indicted are synaptic vesicles (sv), presynaptic membrane (pm), primary cleft (pc) and junctional folds (j).

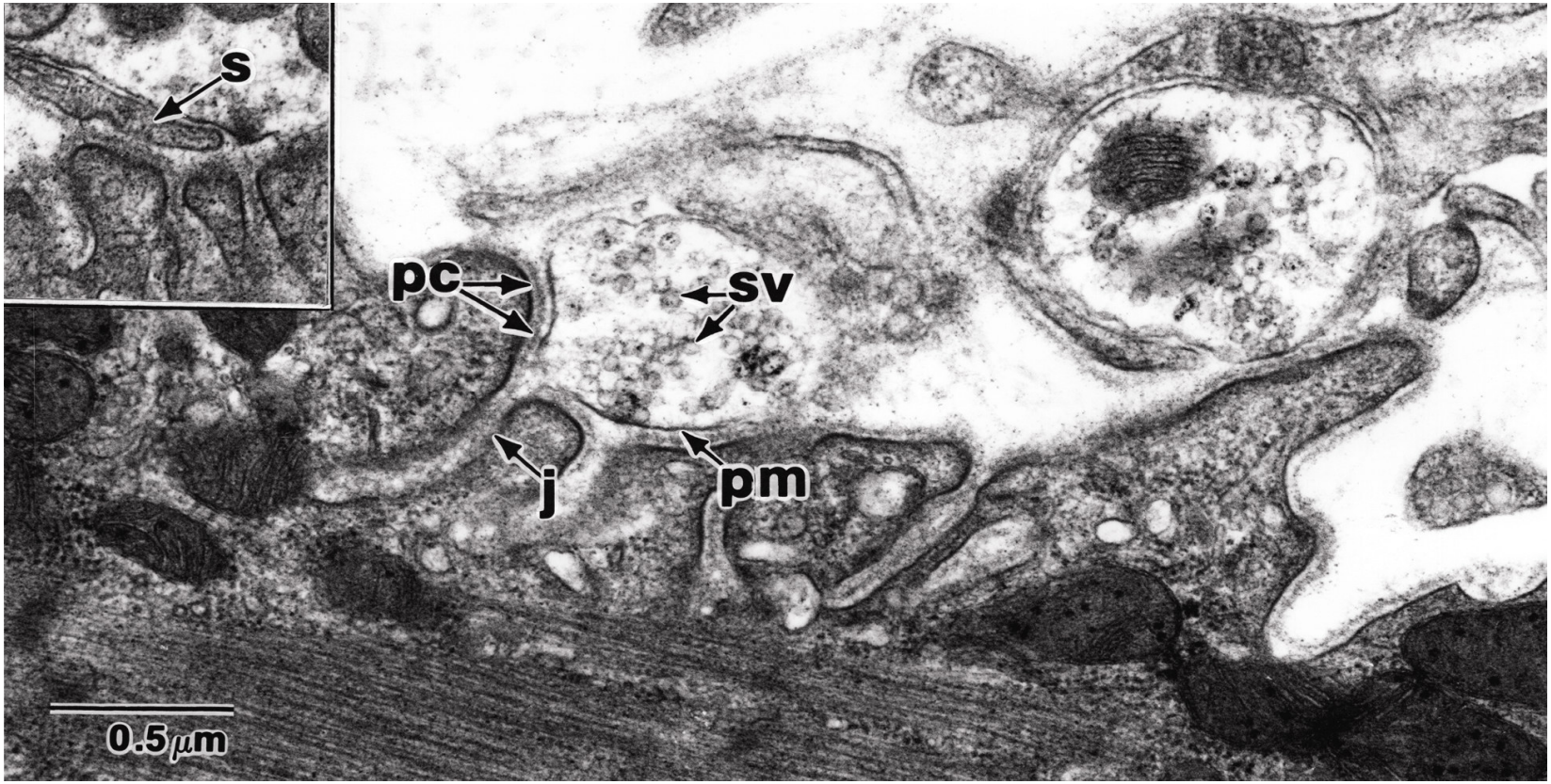

Figure 4B

Figure 4(**B**) Motor endplate from a diaphragm of an AChE -/- mouse. Note Schwann cell process (s) occupying primary cleft. (Inset) 37,000X.

4. Discussion

The present study was undertaken to determine the characteristics of neuromuscular physiology and morphology in AChE -/- mice. Examination of muscle contractility revealed that AChE -/- mice were able to generate sustained neurally elicited tetanic tensions at 70 and 100 Hz, but produced decremental responses at lower and higher stimulation frequencies (Fig. 1). These findings suggest that nullizygous mice had adapted to the absence of AChE, since acute inhibition of AChE leads to a pronounced tetanic fade, which increases progressively with increases in frequency (Adler et al., 2004).

An important adaptation that we identified in a previous study was a reduction in AChR density at the AChE -/- endplate (Adler et al., 2004). Reduction of AChRs would have the effect of accelerating the removal of ACh by diffusion, since the high density of receptors at the endplate acts to retard the efflux of ACh from the synaptic cleft (Katz and Miledi, 1973; Magleby and Pallotta, 1981). Since downregulation of nicotinic AChRs have also been reported to be triggered by chronic exposure to cholinesterase inhibitors (Costa and Murphy, 1983), the loss of AChRs is likely to be a consequence of ACh accumulation. Moreover, Hutchinson et al. (1993) have found similar reductions in AChRs in muscles from patients with congenital human AChE collagen tail deficiency.

Our current TEM study suggests that there is also a reduction in the fraction of the postjunctional membrane that is in contact with the nerve terminal and an overall simplification of the junctional folds (Fig. 4B). It has been estimated that the normal junctional folds, such as those illustrated in Fig. 4A, increase the AChR-containing postsynaptic membrane surface by a factor of 5 (Wood and Slater, 1997). Accordingly, the modified junctional folds of AChE -/- mice would act to reduce the postjunctional surface area and contribute to the lower density of AChRs.

An additional alteration that was prominent in nullizygous mouse endplates was a marked reduction in nerve terminal size (Fig. 4). Terminals appeared to become fragmented such that each presented a smaller region of contact with postjunctional membranes. In many nullizygous endplates, the contact area between pre- and postsynaptic membranes was diminished further by insertion of Schwann cell extensions into the synaptic space (Fig. 4B, inset). Since a nerve terminal that extends over the entire synaptic space acts as a physical barrier to the diffusion of ACh, the presence of smaller terminals would increase diffusion by creating more pathways for the elimination of ACh (Katz and Miledi, 1973). The increased diffusion of ACh would in turn lead to a lower level of receptor desensitization. The presence of more numerous terminals would ensure that the release of ACh would not be diminished and accounts for the findings that both MEPP frequency and *m* were in the normal range (Figs. 2 and 3). The slight decrease in MEPP amplitudes may result from reductions in the ACh content of synaptic vesicles, since the synthesis of ACh would be compromised by a deficiency of choline for uptake due to impaired hydrolysis of ACh (Yu and Van der Kloote, 1991; Gilmore et al., 1996).

The electrophysiological and morphological alterations observed in ACh -/- mice differ markedly from those reported following acute AChE inhibition. The latter results in a striking increase in the amplitude and a marked prolongation in the decay of EPPs and MEPPs (Katz and Miledi, 1973). This contrasts with the slight prolongation of MEPPs and reduction, rather than increase, in their peak amplitude, observed in the present study (Table 2, Fig. 2). Moreover, acute inhibition of AChE produces a focal lesion in the immediate vicinity of the endplate that is

characterized by supercontractions and by swelling of mitochondria and of endoplasmic reticular membranes (Laskowski et al., 1977; Adler et al., 1992). These were clearly not observed in the present study (Fig. 4). The absence of increases in the MEPP amplitude, or of organelle damage, suggests that ACh accumulation is less extensive in AChE -/- muscle than in normal muscle in which AChE activity is acutely inhibited.

In addition to the morphological alterations described above, it is possible that BChE activity also contributes to the maintenance of neuromuscular function. A possible role for BChE is suggested by its apparent synaptic localization (Minic et al., 2003; Girard et al., 2007) and by the finding that the selective BChE inhibitor iso-OMPA enhanced tetanic fade in AChE -/- muscle (Adler et al., 2004). A contribution by BChE activity does not appear to be the case for quantal responses, since iso-OMPA failed to alter MEPPs in either wild-type or nullizygous mice (Fig. 2). BChE is more likely to play a role during repetitive stimulation when ACh concentrations are higher and more sustained (Heffron and Hobbiger, 1979).

This study indicates that reductions in nicotinic AChR density and alterations of synaptic morphology are the principal adaptive responses to chronic excess ACh, and both are suggested to facilitate the diffusion of ACh out of the synaptic cleft. BChE serves to hydrolyze ACh during high frequency stimulation, but does not contribute to the removal of ACh after release of single ACh quanta. This is consistent with findings that BChE does not increase in AChE -/- mice, but rather assumes a latent function that was originally carried out by AChE (Li et al., 2000). The reduced MEPP amplitude in AChE -/- mice (Table 2) suggests that there may also be a decrease in the ACh content of the SSV. Other possible adaptations such as a reduction in the number of quanta released per impulse or a reduction in the desensitization rate of AChRs do not seem to occur (Hutchinson et al., 1993; Minic et al., 2003; Adler et al., 2004). Since the alterations in AChR density and synaptic morphology take time to develop, these adaptations are not possible during acute AChE inhibition, making this condition rapidly fatal.

5. References

Adler, M., Hinman, D. and Hudson, C.S. (1992) Role of muscle fasciculations in the generation of myopathies in mammalian skeletal muscle. Brain Res. Bull. 29, 179-187.

Adler, M., Manley, H.A., Purcell, A., Deshpande, S.S., Hamilton, T.A., Kan, R.K., Oyler, G., Lockridge, O., Duysen, E.G. and Sheridan, R.E. (2004) Reduced acetylcholinesterase receptor density, morphological remodeling, and butyrylcholinesterase activity can sustain muscle function in acetylcholinesterase knockout mice. Nerve & Muscle 30, 317-327.

Adler, M., Petrali, J.P., Moore, D.H. and Filbert, M.G. (1991) Function and distribution of acetyl- and butyrylcholinesterase in canine tracheal smooth muscle. Arch. Int. Pharmacodyn. Ther. 312, 126-139.

Akk, G., Milescu, L.S. and Heckmann, M. (2005) Activation of heteroliganded mouse muscle nicotinic receptors. J. Physiol. 564, 359-376.

Albuquerque, E.X., Pereira, E.F., Aracava, Y., Fawcett, W.P., Oliveira, M., Randall, W.R., Hamilton, T.A., Kan, R.K., Romano, J.A. Jr. and Adler, M. (2006) Effective countermeasure against poisoning by organophosphorus insecticides and nerve agents. Proc. Natl. Acad. Sci. U.S.A. 103, 13220-13225.

Bois, R.T., Hummel, R.G., Dettbarn, W-D. and Laskowski, M. (1980) Presynaptic and Postsynaptic neuromuscular effects of a specific inhibitor of acetylcholinesterase. J. Pharmacol. Exp. Ther. 215, 53 -59.

Brimijoin, S. and Koenigsberger, C. (1999) Cholinesterases in neural development: New findings and toxicologic implications. Environ. Health Perspect. 107 (Suppl. 1), 59-64.

Chatonnet, A. and Lockridge, O. (1989) Comparison of butyrylcholinesterase and acetylcholinesterase. Biochem. J. 260, 625-634.

Colletier, J.P., Fournier, D., Greenblatt, H.M., Stojan, J., Sussman, J.L., Zaccai, G., Sillman, I. and Weik, M. (2006) Structural insights into substrate traffic and inhibition in acetylcholinesterase. EMBO J. 25, 2746-2756.

Costa, L.G. and Murphy, S.D. (1983) [^{3}H]Nicotine binding in rat brain: Alteration after chronic acetylcholinesterase inhibition. J. Pharmacol. Exp. Ther. 226, 392-397.

Del Castillo, J. and Katz, B. (1954) Quantal components of the end-plate potential. J. Physiol. 124, 560-573.

Duysen, E.G., Li, B., Xie, W., Schopfer, L.M., Anderson, R.S., Broomfield, C.A. and Lockridge, O. (2001) Evidence for nonacetylcholinesterase targets of organophosphorus nerve agent: supersensitivity of acetylcholinesterase knockout mouse to VX lethality. J. Pharmacol. Exp. Ther. 299, 528-535.

Duysen, E.G., Stribley, J.A., Fry, D.L., Hinrichs, S.H. and Lockridge, O. (2002) Rescue of the acetylcholinesterase knockout mouse by feeding a liquid diet; phenotype of the adult acetylcholinesterase deficient mouse. Brain Res. Dev. Brain Res. 137, 43-54.

Fiekers, J.F. (1985) Interactions of edrophonium, physostigmine and methanesulfonyl fluoride with the snake end-plate acetylcholine receptor-channel complex. J. Pharmacol. Exp. Ther. 234, 539-549.

Gilmore, M.L., Nash, N.R., Roghani, A., Edwards, R.H., Yi, H., Hersch, S.M. and Levey, A.I. (1996) Expression of the putative vesicular acetylcholine transporter in rat brain and localization in cholinergic synaptic vesicles. J. Neurosci. 16, 2179-2190.

Girard, E., Bernard, V., Minic, J., Chatonnet, A., Krejci, E. and Molgo, J. (2007) Butyrylcholinesterase and the control of synaptic responses in acetylcholinesterase knockout mice. Life Sciences 80, 2380-2385.

Heffron, P.F. and Hobbiger F. (1979) Relationship between inhibition of acetylcholinesterase and response of the rat phrenic nerve-diaphragm preparation to indirect stimulation at higher frequencies. Br. J. Pharmacol. 66, 323-329.

Heuser, J.E., Reese, T.S., Dennis, M.J., Jan, Y., Jan, L. and Evans, L. (1979) Synaptic vesicle exocytosis captured by quick freezing and correlated with quantal transmitter release. J. Cell Biol. 81, 275-300.

Hutchinson, D.O., Walls, T.J., Nakano, S., Camp, S., Taylor, P., Harper, C.M., Groover, R.V., Peterson, H.A., Jamieson, D.G. and Engel, A.G. (1993) Congenital endplate acetylcholinesterase deficiency. Brain 116, 633-653.

Karlin, A. (2002) Emerging structure of the nicotinic acetylcholine receptors. Nat. Rev. Neurosci. 3, 102-114.

Katz, B. and Miledi, R. (1973) The binding of acetylcholine to receptors and its removal from the synaptic cleft. J. Physiol. 231, 549-574.

Laskowski, M.B., Olsen, W.H. and Dettbarn, W-D. (1977) Initial ultrastructural abnormalities at the motor end plate produced by a cholinesterase inhibitor. Exp. Neurol. 57, 13-33.

Li, B., Stribley, J.A., Ticu, A., Xie, W., Schopfer, L.M., Hammond, P., Brimijoin, S., Hinrichs, S.H. and Lockridge, O. (2000) Abundant tissue butyrylcholinesterase and its possible function in the acetylcholinesterase knockout mouse. J. Neurochem. 75, 1320-1331.

Magleby, K.L. and Pallotta, B.S. (1981) A study of desensitization of acetylcholine receptors using nerve-released transmitter in the frog. J. Physiol. 316, 225-250.

Minic, J., Chatonnet, A., Krejci, E. and Molgo, J. (2003) Butyrylcholinesterase and acetylcholinesterase activity and quantal transmitter release at normal and acetylcholinesterase knockout mouse neuromuscular junctions. Br. J. Pharmacol. 138, 177-187.

Miyazawa, A., Fujiyohshi, Y. and Unwin, N. (2003). Structure and gating mechanism of the acetylcholine receptor pore. Nature 423, 949-955.

Rosenberry, T.L., Mallender, W.D., Thomas, P.J. and Szegletes, T. (1999) A steric blockade model for inhibition of acetylcholinesterase by peripheral site ligands and substrate. Chem. Biol. Interact. 119-120, 85-97.

Taylor, P.J. (1991) The cholinesterases. J. Biol. Chem. 266, 4025-4028.

Wood, S.J. and Slater, C.R. (1997) The contribution of postsynaptic folds to the safety factor for neuromuscular transmission in rat fast- and slow-twitch muscles. J. Physiol. 500, 165-176.

Xie, W., Stribley, J.A., Chatonnet, A., Wilder, P.J., Rizzino, A., McComb, R.D., Taylor, P., Hinrichs, S.H. and Lockridge, O. (2000) Postnatal developmental delay and supersensitivity to organophosphate in gene-targeted mice lacking acetylcholinesterase. J. Pharmacol. Exp. Ther. 293, 896-902.

Yu, S.P and Van der Kloot, W. (1991) Increasing quantal size at the mouse neuromuscular junction and the role of choline. J. Physiol. 433, 677-704.

Zimmerman, G. and Soreq, H. (2006) Termination and beyond: acetylcholinesterase as a modulator of synaptic transmission. Cell Tissue Res. 326, 655-969.